

Supplementary Materials

A Circulating Tumor Cell-RNA Assay for Assessment of Androgen Receptor Signaling Inhibitor Sensitivity in Metastatic Castration-Resistant Prostate Cancer

Yu Jen Jan^{1†}, Junhee Yoon^{2†}, Jie-Fu Chen^{1†}, Pai-Chi Teng¹, Nu Yao¹, Shirley Cheng¹, Amber Lozano¹, Gina C.Y. Chu¹, Howard Chung⁷, Yi-Tsung Lu¹, Pin-Jung Chen⁷, Jasmine J. Wang⁷, Yi-Te Lee⁷, Minhyung Kim², Yazhen Zhu⁷, Beatrice S. Knudsen^{3,6}, Felix Y. Feng⁹, Isla P. Garraway⁸, Allen C. Gao¹⁰, Leland W. K. Chung¹, Michael R. Freeman^{2,4,6*}, Sungyong You^{2*}, Hsian-Rong Tseng^{7*}, Edwin M. Posadas^{1,3,5*}

¹ Urologic Oncology Program and Uro-Oncology Research Laboratories, ² Division of Cancer Biology and Therapeutics, Departments of Surgery, ³ Translational Oncology Program, ⁴ Cancer Biology Program, Samuel Oschin Comprehensive Cancer Institute; ⁵ Division of Hematology/Oncology, Department of Medicine, and ⁶ Department of Biomedical Sciences; Cedars-Sinai Medical Center, Los Angeles, California, USA

⁷ Department of Molecular and Medical Pharmacology, California NanoSystems Institute, Crump Institute for Molecular Imaging; ⁸ Department of Urology, David Geffen School of Medicine, University of California, Los Angeles, Los Angeles, California, USA

⁹ Departments of Radiation Oncology, Urology, and Medicine, University of California, San Francisco, San Francisco, California, USA.

¹⁰ Department of Urology, University of California Davis, Davis, CA, USA

† These authors contribute equally to this work.

*Correspondence:

Edwin M. Posadas, MD: edwin.posadas@csmc.edu , +1-310-423-7600

Hsian-Rong Tseng, PhD: HRTseng@mednet.ucla.edu , +1-310-794-1977

Sungyong You, PhD: sungyong.you@cshs.org , +1-310-423-5725

Michael R. Freeman, PhD: michael.freeman@cshs.org , +1-310-423-7069

SUPPLEMENTARY METHODS

Manufacture Materials and Methods of the TR-NanoVelcro CTC Purification System

Fabrication of Silicon Nanowire Substrates (SiNWS)

Silicon wafers (p-type, (100)-orientation, resistivity of ca. 10-20 Ω *cm) were acquired from Silicon Quest International, Inc. (CA, USA). Sulfuric acid (98%), hydrogen peroxide (30%), silver nitrate (>99.8%), hydrofluoric acid (48%), ethanol (>99.5%), and 3-mercaptopropyl trimethoxysilane (95%) were purchased from Sigma-Aldrich Co. (MO, USA). All chemicals were used without additional purification.

Polymer Brush Synthesis and Conjugation

Anhydrous toluene, dichloromethane, N,N-dimethylformamide, triethylamine, 3-aminopropyltriethoxysilane (APTES, 98%), copper(I) bromide (98%), 2-bromo-2-methylpropionyl bromide (98%), N-(3-(dimethylamino)propyl)-N'-ethylcarbodiimide hydrochloride (EDC, \geq 98%), biotin (97%), and 2-aminoethyl methacrylate hydrochloride were obtained from Sigma-Aldrich Co. (MO, USA). N-Isopropylacrylamide (NIPAM, >98.0%) was purchased from Tokyo Chemical Industry Co., Ltd. (TCI) America (OR, USA). All chemicals were used without additional purification.

Fabrication of PDMS Chaotic Mixer

PDMS chaotic mixers were fabricated based on a soft lithographic approach[1, 2]. The patterned silicon master mold (or silicon replicate) was fabricated by a standard two-step photolithographic procedure. A negative photoresist (SU8-2100, MicroChem Corp., MA, USA) was spin-coated with a 100 μ m thickness onto a 3 in. silicon wafer. After exposure to UV and further development, a serpentine fluidic channel with a rectangular cross shape (length 22 cm and width 1.0 mm) was obtained. Another negative photoresist (35 μ m, SU8-2025, MicroChem Corp., MA, USA) was spin-coated on the same wafer. Prior to UV irradiation, the mask was aligned (Karl Suss America Inc., VT, USA) to get an accurate alignment between the prior pattern and the pattern to be imprinted. The fabricated pattern contained ceiling “ridges” that promote chaotic mixing effect in the fluid channel. The mold was then exposed to trimethylchlorosilane vapor for 2-3 min and then transferred to a Petri dish. To prepare a 6-mm thick chip, a well-mixed PDMS prepolymer (GE Silicones, NY, USA; RTV 615 A and B in 10 to 1 ratio) was poured into the mold and kept in an

oven at 80°C for 48 h. The PDMS chaotic mixers were then peeled off from the mold, and two through-holes were punched at the fabric channel's ends for connection with the fluidic handler.

Preparation of Thermoresponsive NanoVelcro Substrates

Photolithography and Wet Etching To Introduce[1, 3] SiNWS onto a Silicon Wafer. Lithographically patterned SiNWS were prepared by a standard photolithography and a chemical wet etching process [4]. Photoresist (AZ 5214) was spin-coated onto a silicon wafer with 100 μm thickness. After exposure of UV light and development, the silicon wafer was kept in etching solution containing deionized water, HF (4.6 M), and silver nitrate (0.2 M). Then, the substrate was treated with boiling aqua regia (3:1 (v/v) HCl/HNO₃) for 15 min. The patterned photoresist on the silicon substrate was removed by rinsing with acetone and ethanol. After being washed with deionized water and then dried with nitrogen, the patterned SiNWS were obtained. Covalently Grafting[5, 6] PIPAAm Polymer Brushes onto SiNWS. The surfaces of the lithographically patterned SiNWS were modified with APTES (1% (v/v) in toluene) to have amine groups. The APTES-grafted SiNWS were reacted with 2-bromo-2-methylpropionyl bromide (9.1 mL, 72 mmol, atom transfer radical polymerization (ATRP) initiator) in the solution of dichloromethane (200 mL) and triethylamine (10 mL, 72 mmol). Then, NIPAM and 2-aminoethyl methacrylate hydrochloride were polymerized on the surface of the ATRP initiator conjugated SiNWS in the presence of Cu(I)Br. PIPAAm containing three different amine group densities (i.e., 2.5, 5.0, and 10.0%) were obtained by controlling the mixing ratios of copolymer precursors. Finally, biotin (0.48 g, 1.9 mmol) was conjugated on PIPAAm-grafted SiNWS via EDC reaction for streptavidin-mediated conjugation of anti-EpCAM.

Analytical validation Studies of the NanoVelcro CTC-RNA Assay and the CTC-PCS1 Panel

We tested a PCa cell line (i.e., 22Rv1) in the NanoVelcro CTC-RNA assay to determine the sensitivity and dynamic range of the assay for measuring CTC-PCS1 RNA signature. We prepared dilutions of 22Rv1 cells with different cell numbers ($n = 5, 10, 50, \text{ and } 100$ cells, mimicking the CTC numbers present in 2-mL clinical blood samples [3, 6-11]) and tested the assay for quantifying RNA transcripts of a housekeeping gene (i.e., HPRT) and the 16 CTC-PCS1 genes. We demonstrated that the NanoVelcro CTC-RNA assay showed high detection sensitivity for quantifying RNA counts of the HPRT gene and the 16 CTC-PCS1 genes at the cell number as low as 5 cells (~100 counts of HPRT and ~1500 total counts in CTC-PCS1 panel genes detected in 5

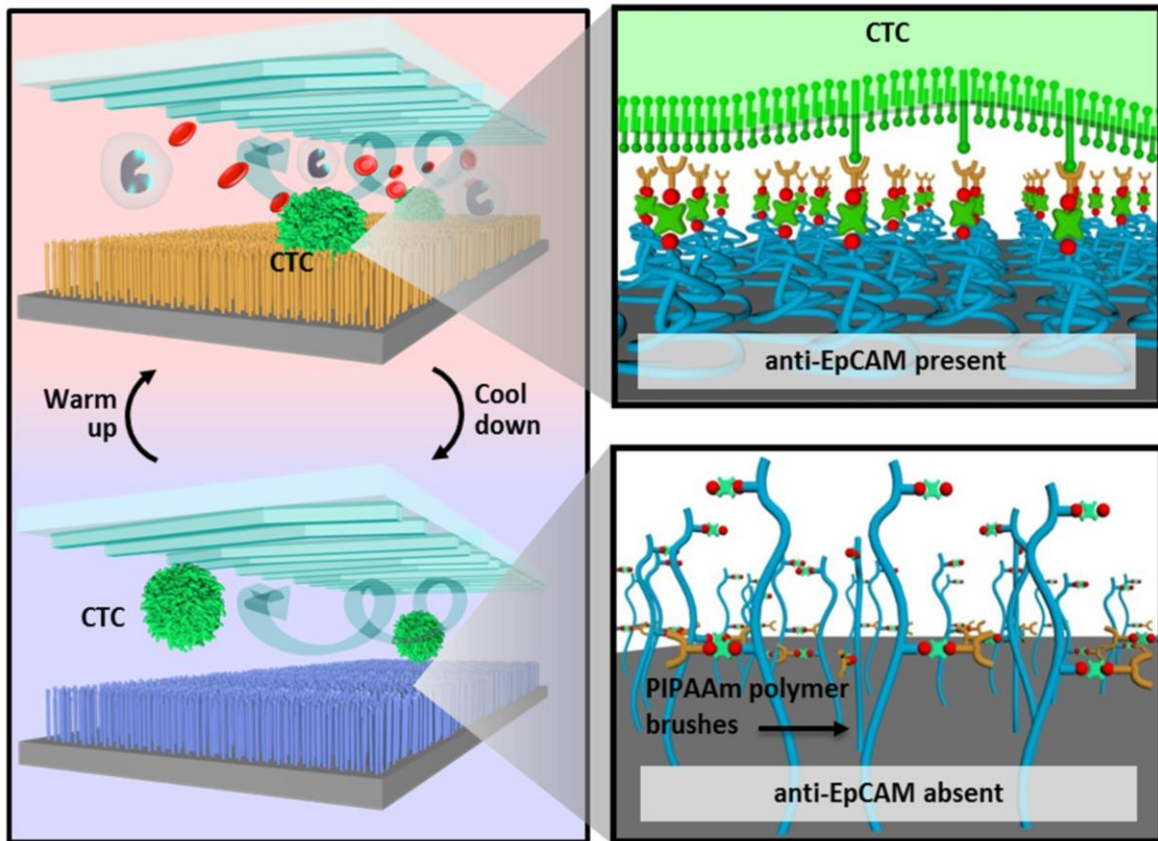
cells, **Supplementary Figure 2A and 2B**). Moreover, the RNA expression detected by our assay showed high linear correlation with 22Rv1 cell numbers (R-square= 0.8298 and 0.8130, respectively). The results indicated that the NanoVelcro CTC-RNA assay exhibited the sensitivity and linearity needed to detect the CTC numbers in the dynamic range of 5-100 cells, which is expected from clinical blood samples.

To demonstrate that the CTC-PCS1 panel detects the CTC-derived PCS1 signatures in the presence of WBC background, we quantified the RNA expression of the CTC-PCS1 panel with NanoString nCounter platform using RNA samples extracted from 2 PCa cell lines (i.e., 22Rv1 and LNCaP) and healthy donor PBMCs. We prepared the samples by extracting RNA from different cell numbers of the PCa cell lines (n = 5, 10, 50, and 100 cells) as well as healthy donor PBMCs (n = 50, 100, 500, and 1000 cells). The cell number ranges mimic the CTC and background WBC numbers (i.e., 5-100 PCa cells and 50-1000 WBCs) observed in the CTC samples purified by the TR-NanoVelcro system [6] from 2-mL of patient blood. We found that the 22Rv1 and LNCaP cells have significantly higher CTC-PCS1 panel gene counts than that of the healthy donor PBMCs in the given dynamic range (**Supplementary Figure 2C**). This was supported by simple linear fitting of the calibration lines. The slopes of curves of 22Rv1 and LNCaP cells are 47 and 44 counts/cell respectively, while the slope of the curve of the healthy donor PBMCs is 3 counts/cell. This result suggested that the CTC-PCS1 panel detects the PCa-specific RNA signature mostly contributed by PCa cells. The RNA expression from background WBCs in the system would have minimal effect to the RNA readout. This further validated the PCa-specific RNA panel selection process of the CTC-PCS1 panel and paved the way for testing in clinical CTC samples with some WBC background.

REFERENCES

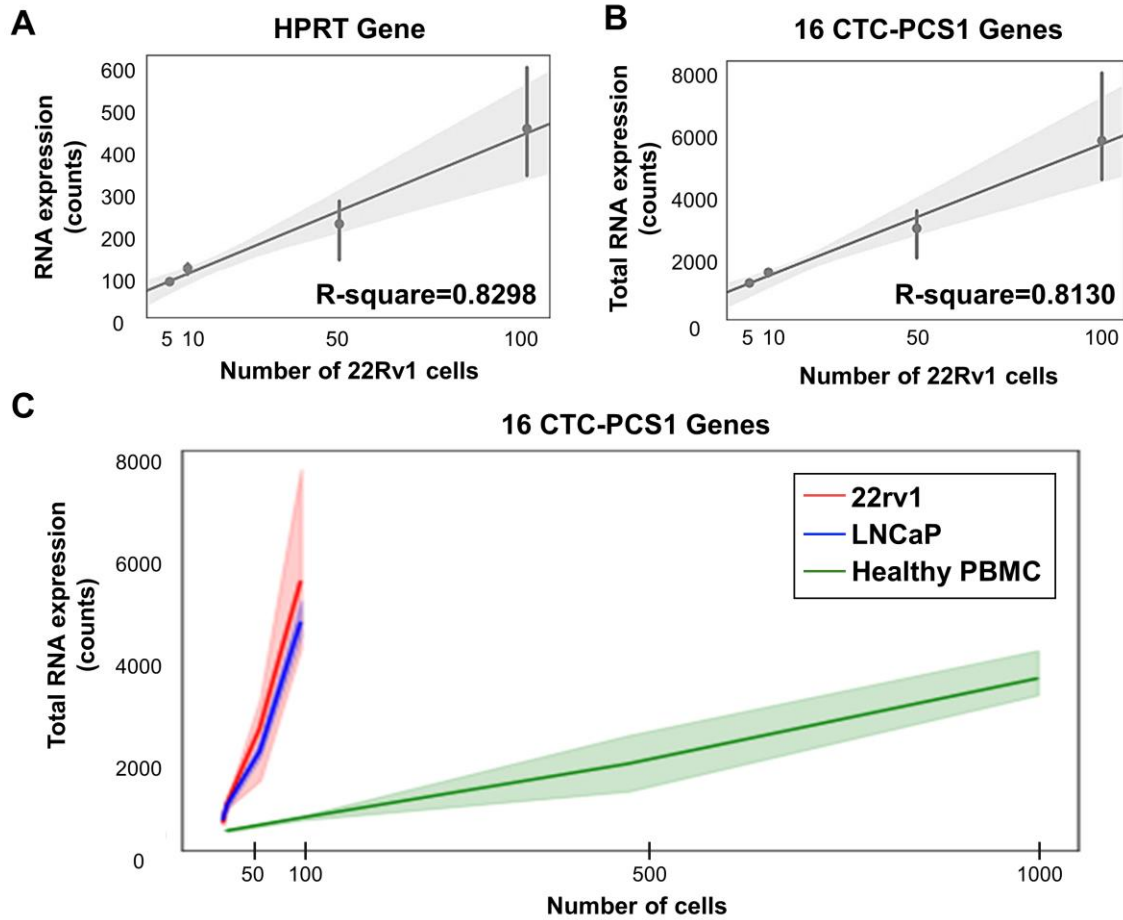
1. Wang S, Liu K, Liu J, Yu ZT, Xu X, Zhao L, et al. Highly efficient capture of circulating tumor cells by using nanostructured silicon substrates with integrated chaotic micromixers. *Angew Chem Int Ed Engl.* 2011; 50: 3084-8.
2. Xia Y, Whitesides GM. SOFT LITHOGRAPHY. *Annu Rev Mater Sci.* 1998; 28: 153-84.
3. Lu YT, Zhao L, Shen Q, Garcia MA, Wu D, Hou S, et al. NanoVelcro Chip for CTC enumeration in prostate cancer patients. *Methods.* 2013; 64: 144-52.
4. Peng KQ, Yan YJ, Gao SP, Zhu J. Synthesis of Large-Area Silicon Nanowire Arrays via Self-Assembling Nanoelectrochemistry. *Adv Mater.* 2002; 14: 1164-7.
5. Hou S, Zhao H, Zhao L, Shen Q, Wei KS, Suh DY, et al. Capture and stimulated release of circulating tumor cells on polymer-grafted silicon nanostructures. *Adv Mater.* 2013; 25: 1547-51.
6. Ke Z, Lin M, Chen JF, Choi JS, Zhang Y, Fong A, et al. Programming thermoresponsiveness of NanoVelcro substrates enables effective purification of circulating tumor cells in lung cancer patients. *ACS Nano.* 2015; 9: 62-70.
7. Lin M, Chen JF, Lu YT, Zhang Y, Song J, Hou S, et al. Nanostructure embedded microchips for detection, isolation, and characterization of circulating tumor cells. *Acc Chem Res.* 2014; 47: 2941-50.
8. Chen J-F, Zhu Y, Lu Y-T, Hodara E, Hou S, Agopian VG, et al. Clinical Applications of NanoVelcro Rare-Cell Assays for Detection and Characterization of Circulating Tumor Cells. *Theranostics.* 2016; 6: 1425-39.
9. Jan YJ, Chen J-F, Zhu Y, Lu Y-T, Chen SH, Chung H, et al. NanoVelcro rare-cell assays for detection and characterization of circulating tumor cells. *Adv Drug Deliv Rev.* 2018 ;125:78-93.
10. Chen JF, Ho H, Lichterman J, Lu YT, Zhang Y, Garcia MA, et al. Subclassification of prostate cancer circulating tumor cells by nuclear size reveals very small nuclear circulating tumor cells in patients with visceral metastases. *Cancer.* 2015;121(18):3240-51
11. Yao N, Jan Y-J, Cheng S, Chen J-F, Chung LWK, Tseng H-R, et al. Structure and function analysis in circulating tumor cells: using nanotechnology to study nuclear size in prostate cancer. *Am J Clin Exp Urol.* 2018; 6: 43-54.

37°C- CTC Capture



4°C- CTC Release

Supplementary Figure 1. The working mechanism of TR-NanoVelcro CTC Purification system. In 37°C, the capture agent (anti-EpCAM) portions of the polymer brush are exposed and CTCs are captured on the thermoresponsive brushes. While the device is cooled down to 4°C, the anti-EpCAM portions of the polymer brush are laid flat and the CTCs are released from the thermoresponsive brushes.



Supplementary Figure 2. Analytical validation studies of the NanoVelcro CTC-RNA assay and CTC-PCS1 panel. (A) The HPRT RNA expression of PCa cell line 22Rv1 in different cell numbers measured by the NanoVelcro CTC-RNA assay (R-square= 0.8298). (B) NanoVelcro CTC-RNA assay quantification of the total CTC-PCS1 panel (16 genes) RNA expression of PCa cell line 22Rv1 in different cell numbers (R-square= 0.8130). (C) The total CTC-PCS1 panel (16 genes) RNA expression directly quantified by NanoString nCounter platform using PCa cell lines 22Rv1, LNCaP and healthy donor PBMCs in different cell numbers. Slopes of the curve- 22Rv1: 47 counts/cell, LNCaP: 44 counts/cell, healthy donor PBMC: 3 counts/cell.

| Patient ID | Sample ID | Age | Race | Treatment | ARSI-S/ ARSI-R | Serum PSA at CTC draw | Disease metastasis sites | Previous CRPC Systemic Treatment |
|------------|-----------|-----|------------------|--------------|-------------------|-----------------------------|-----------------------------|---|
| Patient 1 | Sample 1 | 59 | White | Abiraterone | Sensitive | 0.9 | Bone, Liver | Bicalutamide, Docetaxel |
| Patient 1 | Sample 13 | 59 | White | Abiraterone | Resistant | 7 | Bone, Liver | Bicalutamide, Docetaxel |
| Patient 2 | Sample 4 | 71 | White | Enzalutamide | Sensitive | <0.1 | Lymph node | Bicalutamide, Ketoconazole |
| Patient 2 | Sample 10 | 72 | White | Enzalutamide | Resistant | 3.1 | Lymph node | Bicalutamide, Ketoconazole |
| Patient 3 | Sample 2 | 82 | White | Abiraterone | Sensitive | 676 | Bone, Lymph node | Radium-223, Enzalutamide, Apalutamide |
| Patient 3 | Sample 20 | 83 | White | Abiraterone | Resistant | 2212.6 | Bone, Lymph node | Radium-223, Enzalutamide, Apalutamide |
| Patient 4 | Sample 7 | 73 | White | Enzalutamide | Sensitive | 51.9 | Bone | Bicalutamide, Docetaxel, Abiraterone |
| Patient 4 | Sample 27 | 73 | White | Enzalutamide | Resistant | 185.6 | Bone | Bicalutamide, Docetaxel, Abiraterone |
| Patient 5 | Sample 19 | 75 | White | Abiraterone | Sensitive | 14.7 | Bone | Apalutamide |
| Patient 5 | Sample 11 | 77 | White | Abiraterone | Resistant | 1953.5 | Bone | Apalutamide |
| Patient 6 | Sample 18 | 79 | White | Abiraterone | Sensitive | 713 | Bone | Apalutamide |
| Patient 6 | Sample 26 | 80 | White | Abiraterone | Resistant | 1040 | Bone | Apalutamide |
| Patient 7 | Sample 24 | 71 | White | Enzalutamide | Sensitive | 16.4 | Adrenal gland | None |
| Patient 7 | Sample 30 | 72 | White | Enzalutamide | Resistant | 0.3 | Adrenal gland | None |
| Patient 8 | Sample 25 | 72 | White | Enzalutamide | Sensitive | 1.2 | Lymph node | Bicalutamide, Sipuleucel-T, Abiraterone, Docetaxel |
| Patient 8 | Sample 29 | 73 | White | Enzalutamide | Resistant | 70.6 | Lymph node | Bicalutamide, Sipuleucel-T, Abiraterone, Docetaxel |
| Patient 9 | Sample 3 | 74 | White | Abiraterone | Sensitive | 2.4 | Bone, Lung | Bicalutamide |
| Patient 10 | Sample 5 | 76 | White | Abiraterone | Sensitive | 484.9 | Bone | None |
| Patient 11 | Sample 6 | 62 | White | Abiraterone | Resistant | 2541.1 | Bone, Lymph node, Brain | Apalutamide |
| Patient 12 | Sample 8 | 76 | American Indian | Enzalutamide | Sensitive | 0.1 | Lymph node | Bicalutamide |
| Patient 13 | Sample 9 | 71 | White | Enzalutamide | Sensitive | 0.8 | Bone, Lung | Docetaxel |
| Patient 14 | Sample 12 | 84 | White | Enzalutamide | Resistant | 319.3 | Bone | Ketoconazole, Abiraterone, Radium-223 |
| Patient 15 | Sample 14 | 75 | African American | Abiraterone | Sensitive | <0.1 | Bone, Lymph node | None |
| Patient 16 | Sample 15 | 63 | White | Enzalutamide | Resistant | 14.9 | Lymph node | Bicalutamide, Docetaxel |
| Patient 17 | Sample 16 | 69 | African American | Abiraterone | Sensitive | 14.9 | Bone | Bicalutamide |
| Patient 18 | Sample 17 | 83 | White | Enzalutamide | Resistant | 37.6 | Bone | Bicalutamide |
| Patient 19 | Sample 21 | 75 | American Indian | Enzalutamide | Sensitive | 0.6 | Lymph node | Bicalutamide |
| Patient 20 | Sample 22 | 66 | Asian | Enzalutamide | Sensitive | <0.1 | Bone | None |
| Patient 21 | Sample 23 | 58 | White | Abiraterone | Resistant | 7.8 | Bone, Lung | Bicalutamide |
| Patient 22 | Sample 28 | 81 | White | Enzalutamide | Resistant | 0.2 | Bone | Bicalutamide |
| Patient 23 | Sample 31 | 56 | White | Enzalutamide | Sensitive | 4.1 | Bone, Lymph node | Bicalutamide, Docetaxel |

Supplementary Table 1. Patient demographics. The demographics of total 31 samples from 23 patients. The Patient ID, Sample ID, Age, Race, ARSI Treatment, ARSI-S/ARSI-R status, Serum PSA at CTC draw, Disease metastasis sites and Previous Systemic Treatment are recorded as above.